ISSN: 04532198
Volume 62, Issue 09, October, 2020

Synthesis of High Porous Activated Carbon Nanofibers using the Single-Step Pyrolysis of Reeds Waste and Its Applications in Supercapacitor Electrodes

Rika Taslim[1], Erman Taer[2], Suedi[3], Merry Siska[4], Suwandana[5], Agustino[6], Apriwandi[7]

Department of Industrial Engineering, State Islamic University of Sultan Syarif Kasim, 28293 Simpang Baru, Riau, Indonesia[1,3,4,5]
Department of Physics, University of Riau, 28293 Simpang Baru, Riau, Indonesia[2,6,7]

ABSTRACT— Activated carbon sourced biomass materials widely applied as the energy storage supercapacitors possess high porosity, large specific surface area, controllable surface morphology as well as low-cost. In addition, chemical activation agents are very significant in the process, which are adopted in the opening of active sites and pore structures of activated carbon. This study is aimed at combining a single-step activating process with the carbonization and activation, using KOH, NaOH, and $ZnCl_2$ as agents in the preparation of carbon from low-cost reeds wastes. Furthermore, the resulting thermal stability, density of the electrodes, surface of morphology, microstructure, specific surface area and pore size distribution were investigated. The results show variation in surface area, where the largest was observed in KOH-activated carbon electrode at 1183.540 $m^2\ g^{-1}$, alongside high fibers density and low crystallinity properties. This was followed by the treatment with $ZnCl_2$ and NaOH, showing 768.301 $m^2\ g^{-1}$ and 284.823 $m^2\ g^{-1}$, respectively. Subsequently, the symmetric supercapacitor cells produced with KOH-activated carbon electrode exhibited a high specific capacitance of 141 F g^{-1}, and maximum energy density of 4.89 Wh kg^{-1}, at the power density of 35.32 W kg^{-1}.

KEYWORDS: Reeds waste, activated carbon, carbon nanofiber, electrode material, supercapacitor.

1. INTRODUCTION

Indonesia is a developing country, which is known to rely heavily on primary non-renewable energy sources obtained from fossil fuels, and is expected to run out, alongside the continuous human consumption. According to the Agency for Assessment and Application of Technology, the total energy expended in 2016 was dominated by fuel oil at 47%, with transportation and the industry as the largest usage sectors, at 42% and 36%, respectively. Therefore, a continuous increase in use without changes in pattern, especially in the transportation sector, is expected to disrupt the sustainability and security of energy in Indonesia. According to [1], the use of energy storage devices, including supercapacitors and batteries has enhanced the efficiency of fuel oil use, as seen in electric cars, electric vehicles [2], [3] and trains [4], [5], [6] reviewed the combination of supercapacitors and solar cells, and then demonstrated the system effectiveness and efficiency. These references indicate the possibility for using developed effective energy storage devices and alternative reserves as a substitution to solve the current energy problem, particularly in the field of transportation and industrial technology. Furthermore, supercapacitors are known to be the most widely studied storage device, which possess high capacitance (energy storage value), power density and also long life cycle [7]. These devices also possess the advantage of being very potential, according to [8], due to the very quick storage capacity and the ability to utilize carbon content in the biomass as electrodes. Currently, supercapacitors are widely used in some developed countries, particularly in the field of electronics and transportation systems, as seen in hybrid vehicles, digital cameras, personal memory computers and cellphones, defibrillators, cardiac pacemakers, radars, GSM applications, uninterruptible Power Supply (UPS), and various other functionalities in the fields of medicine, military and industry. Specifically, biomass is also very potential, due to the easy of

acquisition, abundant available quantities, and the relatively affordable prices [9], and is defined as available renewable organic materials, including all natural resources in the form of energy and materials [10]. In addition, previous studies have shown the successful utility of various biomass considered to be weed (pests) as supercapacitors, including rice husk [11], Mission Grass Flower [12], bamboo leaf [13] and others with potentials that have not been research, e.g., reeds (Imperata cylindrica). These are a species of grass in the family Phocaea, known to be widely grown worldwide [14] with the population in Indonesia estimated to reach an area of 8.5 million hectares [15], [6]. Furthermore, they are mostly underutilized, hence regarded as a nuisance plant, which is often destroyed with pesticides or herbicides that possibly cause damage to the soil content. These materials are sometimes cleared with a lawn mower, subsequently incurring additional costs, due to the interestingly high concentration largely spread in most regions. Furthermore, reeds possess active carbon-forming content, encompassing cellulose at 40.22%, hemicellulose 18.40% and lignin 31.29% [17]. These materials have the propensity to serve as large energy storage electrodes, and thus predicted to be very good supercapacitors. This study is, therefore, aimed at producing high porosity and carbon nanofiber densities to support high-performance electrochemical supercapacitors, based on the results that demonstrated a specific surface area of 1138 m^2 g^{-1}.

2. Experimental section

2.1 Synthesis of activated carbon electrodes

The basic materials studied include reeds collected in Riau Province, Indonesia, which was washed to separate the soil, sand and other components. These were subsequently dried to remove a majority of the water content in stage, where the first was performed under the sun for 2 days, and the second required the use of oven set at 110 °C for 48 hours.

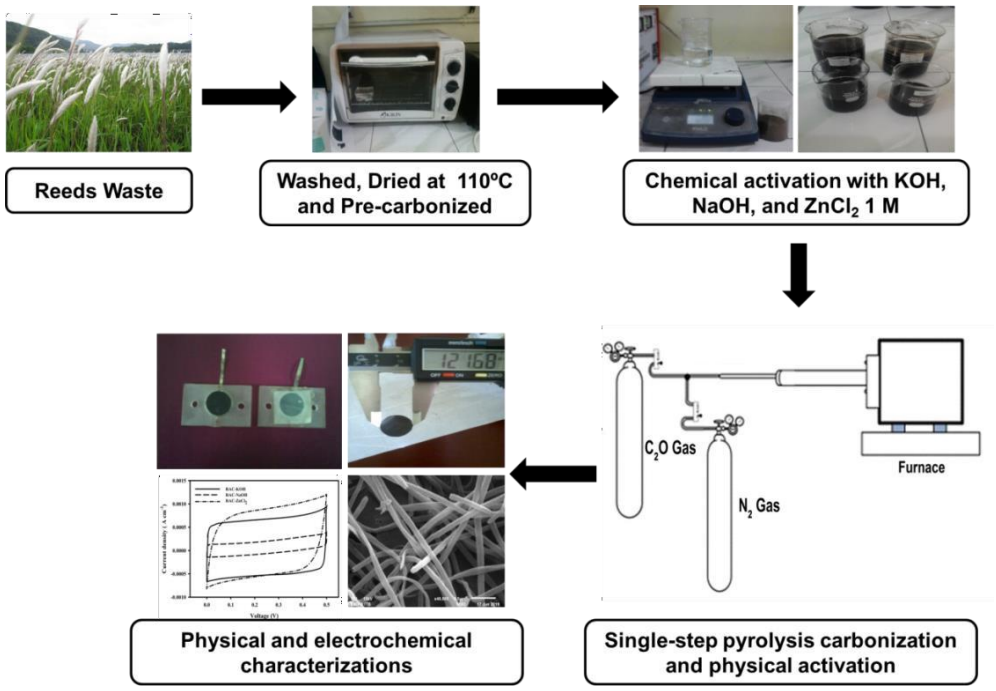

Fig. 1 Schematic preparation of reeds activated carbon electrode

Furthermore, pre-carbonization was performed by heating 45 grams of the sample in a vacuum chamber in phases, initiated with a temperature of 50 °C, which was multiplied every 30 min, up to 250 °C. Subsequently, the samples are manually mashed with mortars, followed by the milling tool, to attain powders, which is mixed with KOH, NaOH and $ZnCl_2$, at 1 M concentration, in a process termed chemical activation. The samples

were then labeled as RAC-KOH, RAC-NaOH, and RAC-$ZnCl_2$, in order to facilitate data analysis, where RAC depicts reeds activated carbon. Therefore, the dried chemically activated carbon powder is converted into a monolith form using a hydraulic press, followed by pyrolysis treatment using single step carbonization initiated with the flow of N2 gas at 600 °C [18]. The next step involves physical activation using CO_2 gas at 850 °C for 2.5 hours, followed by the use of P1200 sand paper to polish the resulting monoliths, and the subsequent neutralization by periodic washing with distilled water. The final stage requires the arrangement of supercapacitor cells in the form of coins' type cell [19], where the electrode components is made from activated carbon, separators, and 1 M H_2SO_4 served as the electrolyte.

2.2 Characterizations

The morphology information and elemental analysis of the reeds activated carbons were characterized using scanning electron microscopy (SEM, JEOL JSM-6510 LA) at a magnification of 5000x, and Energy Dispersive Spectroscopy (EDS, JEOL JSM-6510 LA). Therefore, microstructures analysis involved the use of X-ray diffraction (XRD, X-Pert Pro PW 3060/10) with a Cu k-α 1.5418 Å as a target, and then the pore properties and surface area was characterized using N2 gas adsorption/desorption isotherm (Quantachrome TouchWin v.1.2). Subsequently, the electrochemical performance of all electrode materials were investigated using cyclic voltammetry (CV, CV UR Rad-Er 5841) analysis in a two electrodes system, with a low scanning rate (1 mV/s). The specific capacitance was further calculated using a standard equation [20].

3. Results and Discussion

The thermal stability properties of a material are generally evaluated using Thermogravity Analysis (TGA), which is based on the multi-stage decomposition of mass weight with respect to temperature [21]. The data obtained for the pre-carbonized reed powder are shown in Fig. 2, which illustrates the TG (Thermogravity) profile of mass reduction resulting from increased temperature (ºC), and DTG (Differential Thermal Gravity), which outlines the rate of sample weight loss during the test process from 25 ºC to 600 ºC. In addition, a mass reduction of about 6.02% was observed at 201.4 ºC, indicating the evaporation of H2O and other minerals present in the material, while the highest decline of 44.98% was identified at 350.1 ºC. This phenomenon ensues from the breakdown of complex compounds, in the form of carbon-forming elements present in the powder, encompassing cellulose, hemicellulose and lignin [22-23], which is a very normal event as explained in previous studies. Moreover, further reduction in mass was observed at 550 ºC, indicating the possible decomposition of complex components, e.g., lignin. The DTG profile shows a sharp peak at 325.7 ºC, with a maximum weight loss rate of 0.186 mg/min, indicating the decomposition and simultaneous evaporation of lignocellulose compounds present. This analysis is strengthened by the TG profile, hence the possibility of concluding 325.7 ºC as the thermal stability temperature for reed materials, and the result obtained in this study are consistent with other reports using different materials, including the Husk of babassu coconut and mango pruning [24].

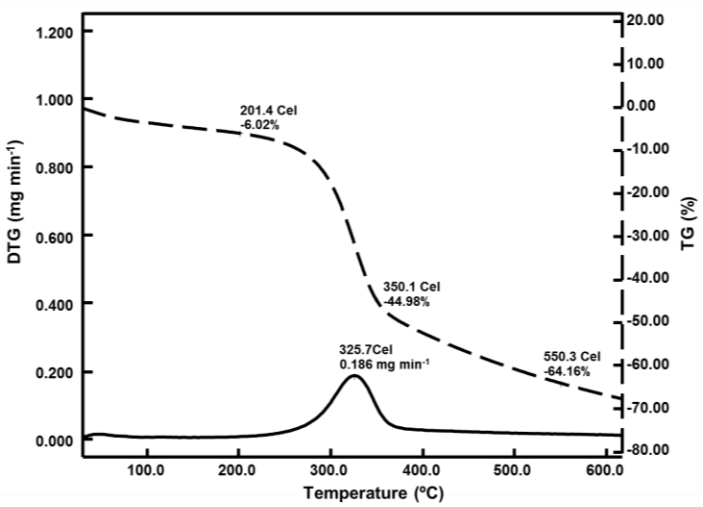

Fig. 2 TG/DTG profile of pre-carbonized reeds powder

The carbon electrode density is a very important characteristic to obtain good capacitance, which is affected by several factors, which consist of the chemical activation and pyrolysis process, including carbonization and physical activation. Furthermore, chemical activators are known to react directly with the carbon powder, while physical activation interacts with the electrode surface, subsequently causing a decline in the density of all sample variations. This effect is indicative of a successful carbonization and activation process in the formation of pores on the electrodes, as the changes observed in reeds carbon electrodes based on different chemical activators are shown in Fig. 3. Specifically, the pyrolysis process perfectly decreases the electrode density, resulting from the ability to breakdown impregnate compounds on the surface, which subsequently forms pores. A similar analysis conducted on coconut shell showed reduction in weight by up to 45%, due to the decomposition and volatile evaporation [25]. Conversely, the KOH activator-based carbon electrode demonstrated the least decline of about 0.63 g cm^{-3}, followed by NaOH and $ZnCl_2$ at 0.75 g cm-3 and 0.65 g cm^{-3}, respectively. Based on this assessment, each chemical activator provides a different effect during the process, as the lowest observed in RAC-KOH correlates with the inherent electrochemical properties, known to be characterized by high specific capacitance. This analysis is fully discussed in the next subsection.

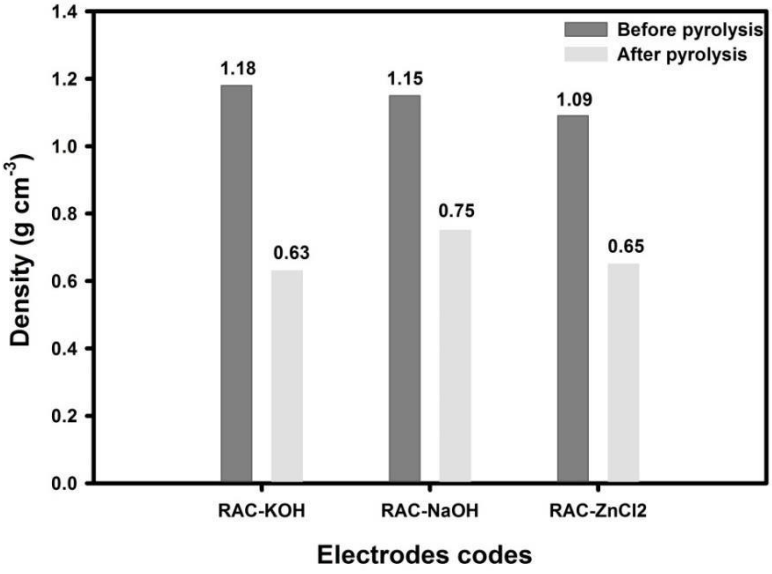

Fig. 3 The Changes in density of reeds carbon electrodes

The crystallinity of KOH, NaOH, and $ZnCl_2$ based reed carbon electrodes was reviewed using the XRD method as shown in Fig. 4, where the spectrum obtained displayed some wide and several sharp peaks. This characteristic pattern depicts the amorphous features of all the electrodes [26], while the two diffraction peaks identified at about 24º and 42º were assigned to (002) and (100/101) graphite carbon reflections, respectively [27]. The appearance observed illustrates the presence of micro-graphite structures, which facilitates the transfer of electrons when used as electrodes' active materials. Particularly, there was no change detected in the 2θ value for the diffraction peak, which verifies the structural reservation after the various activation processes. This data is also similar with other related studies conducted on different biomass that served as the basic activated carbon material, including rice straw, cassava stem, and Oil Palm Kernel Shell [28-30]. In addition, the crystallinity properties were reduced by the NaOH, $ZnCl_2$ and KOH activators, indicated by the XRD pattern expansion in the diffraction peaks at about 24º. Based on strong chemical reactions with carbon atoms, KOH activation was able to produce abundant porous structures [31], while $ZnCl_2$ and NaOH only demonstrated the characteristics of dehydration regents and as templates during the activation process [32-33]. Also the pattern shows several sharp peaks that indicate the presence of other elements, including magnesium, silicon and chlorine. This study outcome is supported by the EDS analysis in the next subsection.

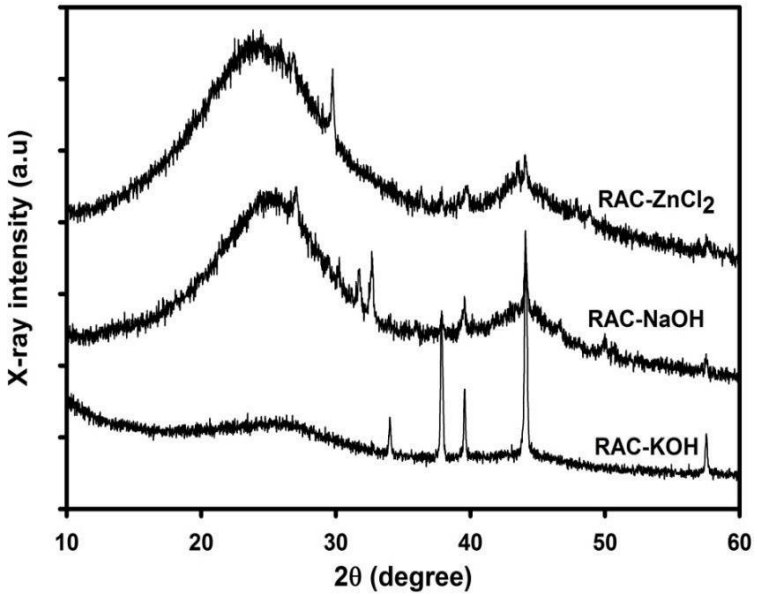

Fig. 4 XRD pattern for RAC-KOH, RAC, NaOH, and RAC-$ZnCl_2$

The X-ray diffraction parameters was determined by using standard equations, including interlayer spacing (d_{002} and d_{100}), calculated based on Bragg's equation, and the microcrystalline dimensions (L_c and L_a), evaluated using the Debye-Scherrer equation. Furthermore, the parameters for all electrodes are shown in Table 1, where all interlayer spacing (d_{002} and d_{100}) appear in normal numbers for biomass material, while the layer height (L_c) and width (L_a) indicate variation in values from one another. Specifically, RAC-KOH demonstrated the smallest L_c at 3.342891, followed by $ZnCl_2$ at 7.050758, and NaOH at 16.05433, and these values are inversely proportional to L_a, which was most significant with the least L_c. The microcrystalline dimensions (L_c and L_a) are known to affect the pore properties, as well as the surface area of carbon electrodes, which is related using the equation SSAxrd = 2/(ρxrdLc) [34-35]. Based on the equation, ρxrd is calculated using the equation $\rho_{xrd} = (d_{002}(\text{graphite})/d_{002})\ \rho\text{graphite})$, with d_{002}(graphite) and ρ(graphite) as 0.33354 nm and 2.268 g cm^{-3}, respectively, hence a high specific surface area is indicated by the low L_c as shown in the RAC-KOH electrodes. This assessment is strengthened by the absorption analysis of N_2 gas in the next subsection.

Table 1. The X-ray parameters for activated carbon reeds

Electrode codes	$2\theta_{002}$ (^{0})	$2\theta_{100}$ (^{0})	d_{002} (Å)	d_{100} (Å)	L_c (Å)	L_a (Å)	L_c/L_a
RAC-KOH	21.557	44.754	4.118972	2.023382	3.342891	63.0078936	0.053055
RAC-NaOH	22.581	44.146	3.934447	2.049828	16.05433	4.639543	3.460326
RAC-$ZnCl_2$	22.475	44.797	3.952763	2.021540	7.050758	17.068225	0.413093

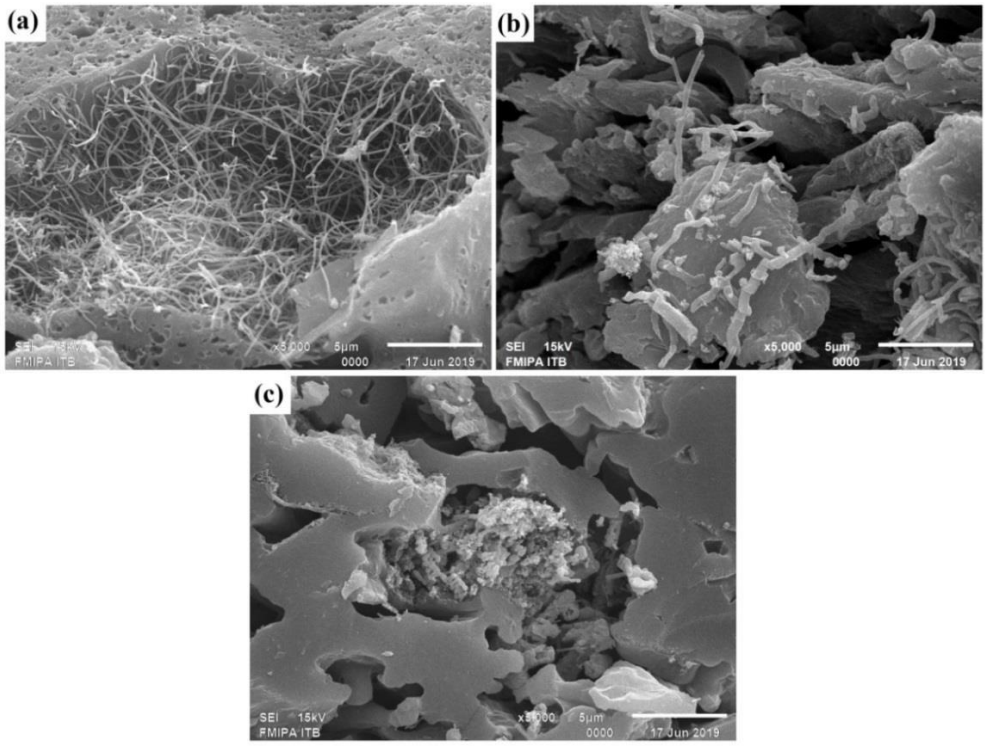

Fig. 5 SEM micrograph with 5000x magnification of activated carbon reeds for a RAC-KOH, b RAC-NaOH, and c RAC-$ZnCl_2$

The surface morphology of the RAC-KOH, RAC-NaOH, and RAC-$ZnCl_2$ electrodes were evaluated using Scanning Electron Microscopy at 5000x magnification, as shown in Fig. 5. This features a variety of structures, which was dependent on the activator agent, as Fig. 5a shows RAC-KOH with high fiber density and small pores, with a diameter range of 90-160 nm and 0.1-0.7 µm, respectively. Furthermore, NaOH activator displays chunks of particles that are large enough, characterized by less dense fiber measuring 1- 3.3 nm in size, and also the visible faults between particles, as shown in Fig. 5b. Fig. 5c shows RAC-ZnCl2 with particle sizes fused through the formation of pores and small particles that almost form fibers. Despite the very fused solid structural appearance, some large enough pores were also observed, in comparison with other small particles within the size range of 100-300 nm, as well as a large number <150 nm. Conversely, fibers are not clearly visible in these particles, possibly due to the nature of the salt ($ZnCl_2$) activator, which affects the carbon structure and forestalls the formation of fibers. Therefore, KOH activator is concluded to be more effective in the process of acquiring high-density fiber structures on reed carbon electrodes, while Fig. 6 shows the SEM micrograph of activated carbon reeds, measured at 40000x magnification.

ISSN: 04532198
Volume 62, Issue 09, October, 2020

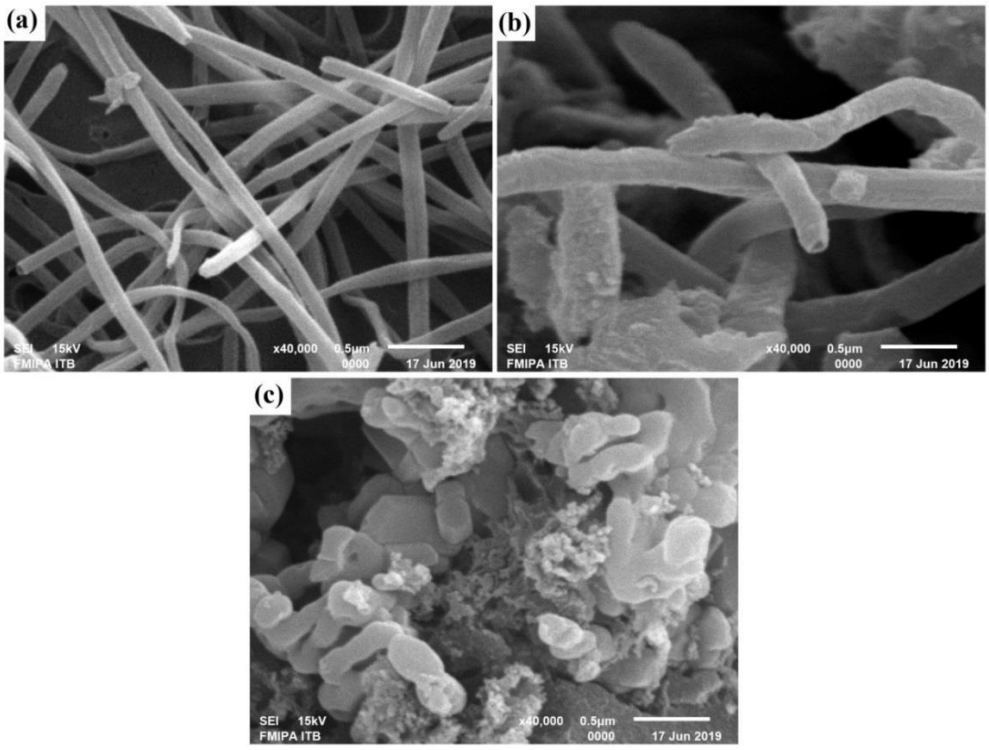

Fig. 6 SEM micrograph with 40000x magnification of activated carbon reeds for a RAC-KOH, b RAC-NaOH, and c RAC-$ZnCl_2$

Table 2. Chemical compositions of reed carbon electrode

Elements	RAC-KOH	RAC-NaOH	RAC-$ZnCl_2$
carbon	89.92	86.51	95.13
Oxygen	8.88	9.84	3.86
Silicon	0.64	0.34	0.56
Clorin	-	0.16	0.11
Pottasium	-	0.24	0.16
Calcium	0,37	0.52	0.18
Iron	-	0.32	-
Magnesium	0,18	-	-
Sulfur	-	1.07	
Natrium	-	1.01	-

The chemical and elemental composition of the reed carbon electrode was analyzed using the Energy Dispersive spectroscopy method. These tend to vary for all samples, depending on each activator agents used, as shown in Table 2, as the carbon element dominates with the highest percentage of 89-95% for each. This was most significant in RAC-$ZnCl_2$ at 95.13%, followed by RAC-KOH and RC-NaOH at 89.92% and 86.51%, respectively. Furthermore, the $ZnCl_2$ activator functions as a de-hydroxylation and dehydration material, prompting the release of hydrogen, oxygen and other complex compounds present at high temperatures, this discharge occurs in the form of steam, in order to obtain electrodes with high carbon elements, which binds very easily with oxygen, subsequently placing it as the second most abundant elements. In addition, several other elements have also been identified, including silica, calcium, potassium and magnesium at relatively low percentages, which exist because of the contribution of the basic biomass material component [36]. This

evaluation confirms previous XRD analysis, characterized by the demonstration of sharp peak on the pattern. The specific surface area and pore structures were investigated using N_2 gas adsorption/desorption analysis, and the isotherms of each fabricated electrode was shown in Fig. 7a. This profile demonstrates the IV type, which is based on IUPAC classification, and indicated by the hysteresis loop in relative pressure of 0.4<P/P0<0.9, which is related by more mesopores [37, 38]. Furthermore, it was established that RAC- NaOH had a low BET specific surface area of 284.823 m^2 g^{-1}, while RAC-$ZnCl_2$ and RAC-KOH were higher at 768.301, and 1183.540 m^2 g^{-1}, respectively. This indicates the propensity for these three activation processes to produce abundant porous structures, with KOH and $ZnCl_2$ demonstrating better pore-forming ability than NaOH, possibly due to differences in mechanisms. Specifically, KOH has strong chemical reactions with the carbon atoms, leading to the production of more porous materials, while ZnCl2 activator functions as de-hydroxylation and dehydration agent, which forms pores as a template for ion diffusion. This result is similarly with the outcome of other studies, where biomass was used as a raw material for activated carbon electrode, as shown in Table 4.

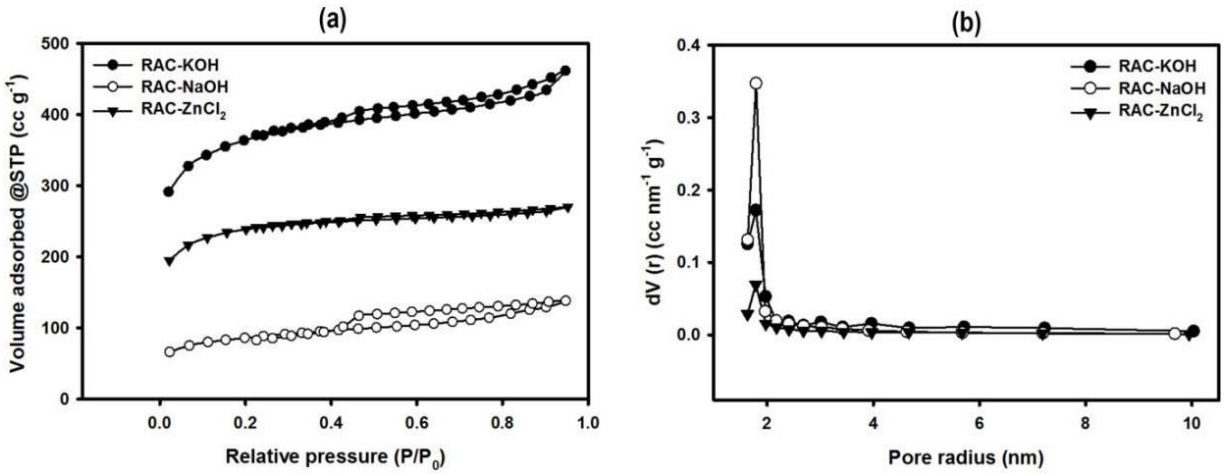

Fig. 7 at The N2 gas adsorption/desorption profile for RACs, b pore distribution of RACs

Fig. 7b shows the absence of micropores in the RAC-KOH, RAC-NaOH, and RAC-ZnCl2 electrodes, as the extent of carbon absorbability is greatly influenced by the state of the pores formed. The mesoporous type pores existing within the range of 1-25 nm were reported in all samples, characterized by medium sizes with a surface area between 1-100 m^3 g^{-1}. These features are known to be good for the activated carbon electrodes of supercapacitors. The cyclic voltammetry is a popular method used to evaluate the specific capacitance of a supercapacitor cell. This procedure was tested on the reed carbon samples in a two electrode system, with a scanning rate of 1 mV s^{-1}, and a voltage window of 0-0.5 V. In addition, 1M H_2SO_4 was selected as the electrolyte, and the CV curve was developed as as a contrast between current density vs. voltage, and the I-V curve for each electrode was shown in Fig. 8. The area of hysteresis is obtained has a directly proportional positive relationship with the specific capacitance [18-19]. Therefore, symmetric rectangular shapes imply quick ion diffusion and good charge propagation at lower scan rate, with Table 3 demonstrating the specific capacitance, energy and power density of the all electrodes.

ISSN: 04532198
Volume 62, Issue 09, October, 2020

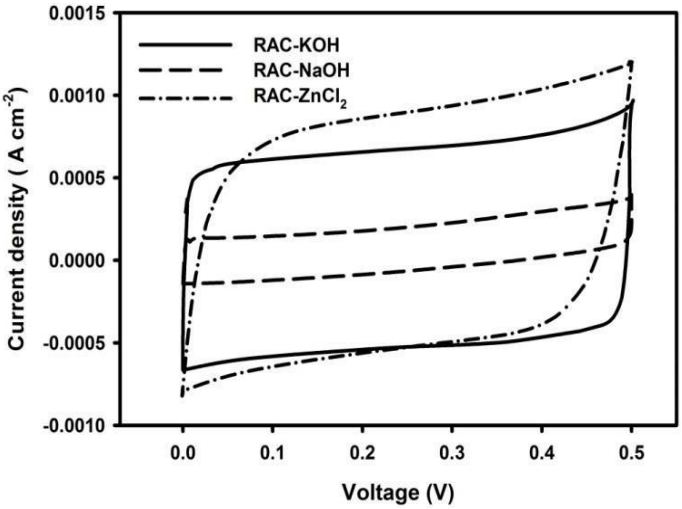

Fig. 8 CV curve for supercapacitor cell

RAC-KOH was observed to possess the highest specific capacitance at 141 F g^{-1}, followed by RAC-$ZnCl_2$ and RAC-NaOH at 124 F g^{-1} and 32 F g^{-1}, respectively. This was due to the relatively high effectiveness in the aspects of increasing the specific capacitance of supercapacitor electrodes created from the reeds. Furthermore, the qualities are supported by the intrinsic physical properties, including the presence of good pore quality, low crystallinity, and high specific surface area, which provides a large medium for ion diffusion into the carbon matrix, and subsequently producing adequate capacitive properties. Based on this analysis, KOH activators were concluded as highly suitable for the meanness of activated carbon electrodes obtained from reed for the purpose of preparing supercapacitor cells, compared with $ZnCl^2$ and NaOH. Table 4 shows a comparison of each activation process of different biomass materials, with respect to specific surface area and specific capacitance

Table 3. The specific capacitance, energy density and power density of reeds activated carbon electrode

Electrodes	C_{sp} (F g^{-1})	E (Wh kg^{-1})	P (W kg^{-1})
RAC-KOH	141	4.89	35.32
RAC-NaOH	32	4.00	28.85
RAC-$ZnCl_2$	124	4.30	31.02

Table 4. Comparison of activation process, specific surface area and specific capacitance of different biomass materials

Biomass materials	Chemical activation	Physical activation	S_{BET} (m^2 g^{-1})	C_{sp} (F g^{-1})	References
Mission grass flower	$ZnCl_2$	CO_2	950	120	[12]
Durian shell	-	H_2O	1889	130	[18]
Pineapple crown	KOH	CO_2	700	150	[19]
Rice straw	KOH	-	1257	137	[28]
Cotton	$ZnCl_2$	N_2	663	240	[32]
Cotton Fiber	NaOH	Ar	584	221	[39]
Cattail	-	CO_2	441	126	[40]
Rubber wood sawdust	-	H_2O	-	93.22	[41]
Durian shell	$ZnCl_2$	H_2O	-	88.39	[42]
Willow leaves	$ZnCl_2$	N_2	1031	216	[43]
Reeds	KOH	CO_2	1183.54	141	This work

4. Conclusion

A single-step carbonization and activation process was proposed for the synthesis of low-cost activated carbon electrode form reeds waste materials, using KOH, NaOH, and $ZnCl_2$ as activating agents. Furthermore, the physical characteristics of the activated carbon were fully analyzed and compared in the aspect of thermal stability, density, microstructure, surface morphology, pore properties and surface area, The RAC-KOH sample demonstrated better electro-capacitive performance, which was mainly due to the reduction of density and crystallinity, high carbon content and nanofiber density, as well as a large specific surface area of about 1183.540 m^2 g^{-1}. In addition, the symmetric supercapacitor cells created using KOH- activated carbon electrode showed a high specific capacitance of 141 F g^{-1} and maximum energy density of 6.94 Wh kg^{-1} at a power density of 350 W kg^{-1}.

5. Acknowledgement

The author is grateful to the LPPM of State Islamic University of Sultan Syarif Kasim, Riau, titled ―study on the use of leaf wastes obtained from the campus environment of UIN SUSKA for the production of electrodes as supercapacitor energy storage devices‖ with contract number: Un.04/L.1/TL.01/445/2019.

6. References

[1] Faggioli, E., Rena, P., Danel, V., Andrieu, X., Mallant, R., Kahlen, H.: Supercapacitors for the energy management of electric vehicles. J. Power Sourc. 84, 261–269 (1999)

[2] Rizoug, N., Mesbahi, T., Sadoun, R., Bartholomeüs, P., Le Moigne, P.: Development of new improved energy management strategies for electric vehicle battery/supercapacitor hybrid energy storage system. Energy Efficiency 11, 823-843 (2018)

[3] Nguyễn, B. H., German, R., Trovão, J. P. F.: Real-Time Energy Management of Battery/Supercapacitor Electric Vehicles Based on an Adaptation of Pontryagin's Minimum Principle. IEEE Transactions on Vehicular Technology 68, 203–212 (2019)

[4] Radu, P. V., Szelag, A., Steczek, M.: On-Board Energy Storage Devices with Supercapacitors for Metro Trains— Case Study Analysis of Application Effectiveness. Energies 12, 1291-1299 (2019)

[5] Yuan, Y., Lu, Y., Jia, B-E., Tang, H., Chen, L., Zeng, Y-J., Hou, Y., Zhang, Q., He, Q., Jiao, L., Leng, J., Ye, Z., Lu, J.: Integrated System of Solar Cells with Hierarchical NiCo2O4 Battery-Supercapacitor Hybrid Devices for Self-Driving Light-Emitting Diodes. Nano-Micro Lett. 11, 42-50 (2019)

[6] Vega-Garita, V., Ramirez-Elizondo, R., Narayan, N., Bauer, P.: Integrating a photovoltaic storage system in one device: A critical review. Prog. Photovolt. Res. Appl. 27, 346–370 (2019)

[7] Gao, Y.: Graphene and Polymer Composites for Supercapacitor Applications: a Review. Nanoscale Res. Lett. 12, 387-385 (2017)

[8] Berenguer, R.: Trends and research challenges in supercapacitors. Bol. Grupo Español Carbón (2015) http:// www.gecarbon.org/boletines/ articulos/BoletinGEC_037_art3.pdf

[9] González, A., Goikolea, E., Barrena, J. A., Mysyk, R.: Review on supercapacitors: Technologies and materials. Renew. Sustain. Energy Rev. 58, 1189–1206 (2016)

[10] Abioye, A. M., Ani, F. N.: Recent development in the production of activated carbon electrodes from agricultural waste biomass for supercapacitors: A review. Renew. Sustain. Energy Rev. 52, 1282–1293 (2015)

[11] Liu, D., Zhang, W., Huang, W.: Effect of removing silica in rice husk for the preparation of activated carbon for supercapacitor applications. Chinese Chem. Lett. 30, 1315-1319 (2019)

[12] Taer, E., Yusra, E., Taslim, R., Mustika, W. S., Nurjanah, S., Yani, R. I., Sari, Y. P., Awitdrus, Apriwandi, Agustino, Tahir, D.: Preparation of Mission Grass Flower-Based Activated Carbon Monolith Electrode for Supercapacitor Application. Int. J. Electrochem. Sci. 14, 7317–7331 (2019)

[13] Yang, F., Zhang, X., Yang, Y., Hao, S., Cui, L.: Characteristics and supercapacitive performance of nanoporous bamboo leaf-like CuO. Chem. Phys. Lett. 691, 366–372 (2018)

[14] Hidayat, S., Bakar, M. S. A., Yang, Y., Phusunti, N., Bridgwater, A.V.: Characterisation and Py-GC/MS analysis of Imperata Cylindrica as potential biomass for bio-oil production in Brunei Darussalam. J. Analytical and Appl. Pyrolysis 134, 510 (2018)

[15] Garrity, D. P., Soekadi, M., Van, N., la Cruz, M. D., Pathak, P., Gunasena, H., Van, S., Huijun, G., Majid, N.: The Imperata Grasslands of TropicalAsia: Area, Distribution, and Typology. Agroforestry Systems 36, 3-29 (1997)

[16] Sutiya, B., Wiwin, T. I., Adi, R., Sunardi.: Kandungan Kimia dan Sifat Serat Alang-Alang (Imperata Cylindrica) Sebagai Gambaran Bahan Baku Pulp dan Kertas. Bioscientiae 9, 8-19 (2012)

[17] Kartikasari, S. D., Nurhatika, S., Muhibuddin, A.: Potensi Alang-alang (Imperata cylindrica (L.) Beauv) dalam Produksi Etanol Menggunakan Bakteri Zymomonas mobilis. jurnal sains dan seni pomits 2, 2337-3520 (2013)

[18] Taer, E., Apriwandi, A., Taslim, R., Malik, U.: Single step carbonization-activation of durian shells for producing activated carbon monolith electrodes. Int. J. Electrochem. Sci. 14, 1318-1330 (2019)

[19] Taer, E., Apriwandi, A., Ningsih, Y. S., Taslim, R., Agustino.: Preparation of activated carbon electrode from pineapple crown waste for supercapacitor application Int. J. Electrochem. Sci. 14, 2462-2475 (2019)

[20] Ma, X., Ding, C., Li, D., Wu, M., Yu, Y.: A facile approach to prepare biomass-derived activated carbon hollow fibers from wood waste as high-performance supercapacitor electrodes. Cellulose 25, 4743–4755 (2018)

[21] Strezov, V., Moghtaderi, B., Lucas, J. A.: Computational calorimetric investigation of the reactions during thermal conversion of wood biomass. Biomass and Bioenergy (2004) doi: 10.1016/j.biombioe.2004.04.008

[22] Wilson, L., Yang, W., Blasiak, W., Jonh, G. R., Mhilu, C.: Thermal characterization of tropical biomass feedstocks. Energy Conversion and Management 52, 191–198 (2011)

[23] Strandberg, A., Holmgren, P., Broström. M.: Predicting fuel properties of biomass using

thermogravimetry and multivariate data analysis. Fuel Process. Technol. 156:107–12. (2017)

[24] de Luna, M. Y., Rodrigues, P. M., Torres, G. A. M., da Costa, J. A. E., Queiroz, M. J., Elaine, M. S., Alexsandra de Sousa, R. M.: A thermogravimetric analysis of biomass wastes from the northeast region of Brazil as fuels for energy recovery. Energy Sources, Part A: Recovery, Utilization, and Environmental Effects 12, 1557-1572 (2018)

[25] Katesa, J., Junpiromand, S., Tangsathitkulchai, C.: effect of carbonization temperature on properties of char and activated carbon from coconut shell. Suranaree J. Sci. Technol. 20, 269-278 (2013)

[26] González, J. F., Román, S., Encinar, J. M., Martínez, G. J.: Pyrolysis of various biomass residues and char utilization for the production of activated carbons. Anal. Appl. Pyrolysis 85, 134-141 (2009)

[27] Wang, Q., Liang, X., Qiao, W., Liu, C., Liu, X., Zhan, L., Ling, L.: Preparation of polystyrene-based activated carbon spheres with high surface area and their adsorption to dibenzothiophene Fuel Process. Technol. 90, 381 (2009)

[28] Liu, S., Zhao, Y., Zhang, B., Xia, H., Zhou, J., Xie, W., Li, H.: Nano-micro carbon spheres anchored on porous carbon derived from dual biomass as high rate performance supercapacitor electrodes. J. Power Sourc. 381, 116– 126 (2018)

[29] Sulaiman, N. S., Danish, M., Hashim, R., Amini, M. H. M., Sulaiman, O.: Optimization of activated carbon preparation from cassava stem using response surface methodology on surface area and yield. J. Cleaner Product. 198, 1422-1430 (2018)

[30] Misnon, I. I., Zain, N. K. M., Jose, R.: Conversion of Oil Palm Kernel Shell Biomass to Activated Carbon for Supercapacitor Electrode Application, New Carbon Mater. 32, 592 (2017)

[31] Zhang, Z., Li, X., Huang, J., Xing, W., Yan, Z.: Functionalization of petroleum coke-derived carbon for synergistically enhanced capacitive performance Nanoscale Res. Lett., 11, 1 (2016)

[32] Q. Sun, T.Jiang, G. Zhao, J. Shi, Int. J. Electrochem. Sci. 14, 1 (2019)

[33] Chiu, Y-H., Lin, L-Y.: Effect of activating agents for producing activated carbon using a facile one-step synthesis with waste coffee grounds for symmetric supercapacitors. J. Taiwan Institute of Chemical Engineers 101, 177 (2019)

[34] Kumar, K., Saxena, R. K., Kothari, R., Suri, D. K., Kaushik, N. K., Bohra, J. N.: Correlation between adsorption and x-ray diffraction studies on viscose rayon based activated carbon cloth. Carbon 35, 1842–1844 (1997)

[35] Deraman, M., Daik, R., Soltaninejad, S., Nor, N. S. M., Awitdrus, Farma, R., Mamat, N. F., Basri, N. H., Othman, M. A. R.: A new empirical equation for estimating specific surface area of supercapacitor carbon electrode from X-ray diffraction. Adv. Mater. Res. 1108, 1-7 (2015)

[36] Saidur, R., Abdelaziz, E. A., Demirbas, A., Hossain, M. S., Mekhilef, S.: A review on biomass as a fuel for boilers Renew. Sustain. Energy Rev. 15, 2262-89 (2015)

[37] Sing, W. S. K., Everett, H. D., Haul, W. A. R., Moscou, L., Pierotti, A. R., Rouquerol, J., Siemieniewska, T.: Reporting physisorption data for gas/solid systems with special reference to the determination of surface area and porosity. Pure and Applied Chemistry 57, 603-619 (1985)

[38] Inagaki, M., Konno, H., Tanaike, O.: Carbon materials for electrochemical capacitors J. Power Sourc. 195, 7880- 7963 (2010)

[39] Liu, Y., Shi, Z., Gao, Y., An, W., Cao, Z.: Biomass-swelling Assisted Synthesis of Hierarchical Porous Carbon Fibers for Supercapacitor Electrodes. ACS Appl. Mater. Inter. 8, 283-291 (2016)

[40] Yu, M., Han, Y., Li, J., Wang, J.: CO2-activated porous carbon derived from cattail biomass for removal of malachite green dye and application as supercapacitors Chem. Eng. J. 317, 493–502 (2017)

[41] Taer, E., Apriwandi, Yusriwandi, Mustika, W. S., Zulkifli, Taslim, R., Sugianto, Kurniasih, B., Agustino, Dewi, P.: Comparative study of CO2 and H2O activation in the synthesis of carbon electrode for supercapacitors. AIP Conference Proceedings 1927, 030036 (2018).

[42] Taer, E., Dewi, P., Sugianto, Syech, R., Taslim, R., Salomo, Susanti, Y., Purnama, A., Apriwandi, Agustino, Setiadi. R. N: The synthesis of carbon electrode supercapacitor from durian shell based on variations in the activation time. AIP Conference Proceedings 1927, 030026 (2018)

[43] Liu, Y., Wang, Y., Zhang, G., Liu, W., Wang, D., Dong, Y.: Preparation of activated carbon from willow leaves and evaluation in electric double-layer capacitors. Mater. Lett. 176, 60-67 (2016)